Bis(benzimidazolyl)amine copper complexes with a synthetic 'histidine brace' structural motif relevant to polysaccharide monooxygenases

ARTICLE *in* INORGANICA CHIMICA ACTA · OCTOBER 2014

Impact Factor: 2.05 · DOI: 10.1016/j.ica.2014.06.027

4 AUTHORS, INCLUDING:

Ivan Castillo
Universidad Nacional Autónoma de México
44 PUBLICATIONS **309** CITATIONS
SEE PROFILE

Erica Zeglio
Linköping University
4 PUBLICATIONS **13** CITATIONS
SEE PROFILE

Inorganica Chimica Acta 422 (2014) 152–157

Contents lists available at ScienceDirect

Inorganica Chimica Acta

journal homepage: www.elsevier.com/locate/ica

Bis(benzimidazolyl)amine copper complexes with a synthetic 'histidine brace' structural motif relevant to polysaccharide monooxygenases

Ivan Castillo [a,*], Andrea C. Neira [a], Ebbe Nordlander [b], Erica Zeglio [b]

[a] Instituto de Química, Universidad Nacional Autónoma de México, Circuito Exterior, CU, México DF 04510, Mexico
[b] Inorganic Chemistry Research Group, Chemical Physics, Center for Chemistry and Chemical Engineering, Lund University, Box 124, SE-221 00 Lund, Sweden

ARTICLE INFO

Article history:
Received 9 May 2014
Received in revised form 27 June 2014
Accepted 28 June 2014
Available online 5 July 2014

Dedicated to Don Tilley

Keywords:
Copper complexes
Benzimidazoles
X-ray crystal structures
Tridentate ligands

ABSTRACT

Reaction of Cu^{2+} salts with the benzimidazole-*N*-methylated bis[(1-methyl-2-benzimidazolyl)ethyl]amine ligand **2BB** results in either bi- or monometallic complexes. Spectroscopic and solid state characterization reveals either square pyramidal or trigonal bipyramidal coordination geometries around the cupric ions. In **[{2BBCu(μ-F)}$_2$](BF$_4$)$_2$**, the dicopper structure is determined by the bridging nature of the fluoro ligands, which complement the T-shape arrangement of N_3 donors provided by **2BB** to define a square pyramidal (or capped distorted tetrahedral) coordination geometry. The monocopper complexes **2BBCuCl$_2$** and **[2BBCu(H$_2$O)$_2$](OTf)$_2$** are characterized by a trigonal bipyramidal geometry both in solution and in the solid state. In all complexes, the T-shape N_3 donor set of **2BB** is analogous to the coordination environment of the copper ions provided by a 'histidine brace' and an additional histidine imidazole in the active site of polysaccharide monooxygenases.

1. Introduction

Nitrogen-containing heterocycles represent an important class of compounds due to their σ-donor and π-acceptor properties towards transition metals, which can be tuned based on the identity of the heterocycle. For example, the imidazole heterocycle of histidine is ubiquitous in nature for transition metal binding in metalloenzyme active sites, conferring the metal centers specific properties. In this context, chemical and biochemical oxidations promoted by the $Cu^{2+/+}$ redox couple are the subject of intense research due to their involvement in the selective oxidation of a wide range of organic substrates [1]. In the case of copper-dependent metalloenzymes, the study of their remarkable selectivity has been aided by the development of synthetic models, which facilitate understanding of the factors that govern the intimate details of dioxygen activation and subsequent substrate oxidation. Although imidazole would appear as the ideal choice of nitrogen heterocycle for the development of model complexes, most examples incorporate pyrazolyl- [2], pyridyl- [1c,3], and amine-based ligands [1,4], perhaps due to their synthetic accessibility. In this context, we have recently exploited 2-substituted benzimidazoles to assemble chelating ligands for $Cu^{2+/+}$ complexes, based on the pK_a value of protonated 2-methylbenzimidazole (6.10) [5], as well as its association constant with Cu^{2+} (log K 4.43) [6], relative to the values reported for histidine (pK_a 6.17, log$K$ not comparable due to chelate formation) [7].

Reports on chelating ligands for copper complexes based on benzimidazoles remain relatively scarce [8], with the notable exception of the binucleating scaffolds developed by Casella, Costas and coworkers [9]. Nonetheless, the chemistry of benzimidazole-based ligands appears to be maturing at a fast pace, as evidenced in the growing number of reports that exploit their properties as versatile N-donors [10]. Our contribution to this area has involved the development of biologically-inspired copper systems with 2-substituted benzimidazoles as platforms for tripodal tetradentate ligands [11]. As an extension to this approach, our attention has now focused on the recently described lytic polysaccharide monooxygenases (PMOs) [12], including the auxiliary activity (AA) family of copper-dependent enzymes [13], which feature a conserved type-2 binding site with an N_3 donor set defined by two histidine imidazoles, as well as a backbone nitrogen from one of the histidine residues in the structural motif known as the 'histidine brace' (Scheme 1) [13a,14]. These enzymes oxidatively cleave recalcitrant polysaccharides, with potential applications in biomass conversion. The bis[(1-methyl-2-benzimidazolyl)ethyl]amine **2BB** in Scheme 1 represents a viable candidate for spectroscopic and structural studies of copper complexes as a first approximation to model systems inspired on the mononuclear active sites of PMOs; our interest was further spurred by the methylated nitrogen atom in one of the histidine imidazoles [13a], since **2BB** consist of methylated benzimidazole moieties. Thus, we

* Corresponding author. Fax: +52 55 56162217.
E-mail address: joseivan@unam.mx (I. Castillo).

http://dx.doi.org/10.1016/j.ica.2014.06.027
0020-1693/

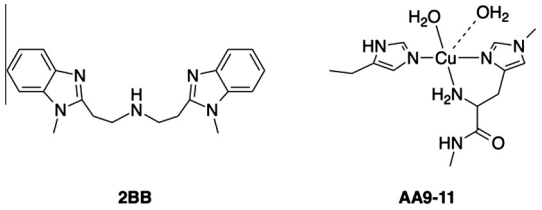

Scheme 1. Ligand employed (**2BB**) and active site of polysaccharide monooxygenases AA9–AA11.

herein report our initial findings on the reactivity of the **2BB**/Cu^{2+} system.

2. Experimental

2.1. Reagents and techniques

Solvents and reagents were obtained from commercial suppliers, and were used without further purification. Ligand **2BB** was prepared according to the literature procedure [15]. Infrared spectra were obtained with a Perkin Elmer 203-B spectrometer in the range 4000–400 cm^{-1} as KBr disks. Mass spectra were obtained on a JEOL JMS-SX-102A mass spectrometer at an accelerating voltage of 10 kV, with a nitrobenzyl alcohol matrix and Xenon atoms at 6 keV (FAB), or a Bruker Daltonics Esquire 6000 spectrometer with ion trap (Electrospray). Melting points were determined on an Electrothermal Mel-Temp apparatus and are uncorrected.

2.2. Synthetic procedures

[{2BBCu(μ-F)}$_2$](BF$_4$)$_2$: *General procedure for complex synthesis:* to a solution of **2BB** (150 mg, 0.45 mmol) in 10 mL methanol was added $Cu(BF_4)_2{\cdot}6H_2O$ (155 mg, 0.45 mmol), and the mixture was heated to reflux for 4 h. After cooling to room temperature a green solid started to deposit, volatiles were evaporated under reduced pressure, and the resulting solid was washed with 2 × 10 mL of diethyl ether to afford **[{2BBCu(μ-F)}$_2$](BF$_4$)$_2$** in 82% yield (186 mg). Mp. 188–190 °C; IR (KBr): 3417, 3132, 3054, 2934, 2902, 2862, 1613, 1518, 1490, 1457, 1411, 1358, 1330, 1295, 1259, 1237, 1182, 1149, 1123, 1091, 1028, 1007, 931, 862, 829, 763, 563, 505, 435. ESI MS: *m*/*z* 396 **[2BBCu]**$^+$. UV–Vis (methanol): 245 (14 530), 272 (15 730), 279 (15 490), 720 (255), 952 (123). *Anal.* Calc. for $C_{40}H_{46}B_2Cu_2F_{10}N_{10}$ **[[{2BBCu(μ-F)}$_2$](BF$_4$)$_2$]**·$2H_2O$ (%): C, 46.12; H, 4.84; N, 13.45. Found: C, 45.97; H, 4.34; N 13.29%.

[2BBCuCl$_2$]: **2BB** (150 mg, 0.45 mmol) in 10 mL methanol was added $CuCl_2{\cdot}2H_2O$ (77 mg, 0.45 mmol), Yield 78% (164 mg). Mp. 198–200 °C; IR (KBr): 3180, 3056, 2929, 2884, 1612, 1495, 1456, 1413, 1361, 1329, 1292, 1237, 1193, 1152, 1127, 1095, 1029, 1008, 976, 932, 861, 828,761, 567, 505, 438. FAB MS: *m*/*z* 396 **[2BBCu]** $^+$. UV–Vis (methanol): 245 (39 900), 272 (43 450), 279 (43 340), 723 (157), 960 (124). *Anal.* Calc. for $C_{20}H_{23}Cl_2CuN_5$ **[2BBCuCl$_2$]** (%): C, 51.34; H, 4.95; N, 14.97. Found: C, 50.92; H, 4.55; N 14.61.

[2BBCu(H$_2$O)$_2$](OTf)$_2$: **2BB** (150 mg, 0.45 mmol) in 10 mL methanol was added $Cu(OTf)_2{\cdot}6H_2O$ (201 g, 0.45 mmol), Yield 97% (319 mg). Mp. 198–200 °C; IR (KBr): 3356, 3241, 2953, 1640, 1617, 1500, 1459, 1415, 1331,1283, 1229, 1153, 1088, 1027, 976, 935, 859, 750, 632, 571, 514, 436. FAB MS: *m*/*z* 545 **[2BBCu(OTf)]**$^+$, 396 **[2BBCu]**$^+$. UV–Vis (methanol): 247 (50,500), 272 (55,940), 279 (55,280), 722 (82), 966 (62). *Anal.* Calc. for $C_{22}H_{27}CuF_6N_5O_8S_2$ **[[2BBCu(H$_2$O)$_{1.5}$](OTf)$_2$]** (%): C, 36.59; H, 3.63; N, 9.70. Found: C, 37.14; H, 4.04; N 9.76%.

2.3. EPR spectroscopy

EPR measurements were made at room temperature or 77 K in quartz tubes with a Jeol JES-TE300 spectrometer operating at X band frequency (9.4 GHz) at 100 kHz field modulation, with a cylindrical cavity (TE_{011} mode); spectra were acquired in the solid state and in frozen acetonitrile or acetonitrile/dichloromethane solutions. The external measurement of the static magnetic field was made with a precision gaussmeter Jeol ES-FC5. Spectral acquisition, manipulations, and simulations were performed using the program ESPRIT-382, v1.916.

2.4. X-ray crystallography

Selected crystallographic data are presented in Table 1. Single crystals were mounted on a Bruker SMART diffractometer equipped with an Apex CCD area detector. Frames were collected by omega scans, and integrated with the Bruker SAINT software package using the appropriate unit cell [16]. The structures were solved using the SHELXS-97 program [17], and refined by full-matrix least-squares on F^2 with SHELXL-97 [18]. Weighted *R*-factors, R_w, and all goodness of fit indicators, *S*, were based on F^2. The observed criterion of ($F^2 > 2\sigma F^2$) was used only for calculating the *R*-factors. All non-hydrogen atoms were refined with anisotropic thermal parameters in the final cycles of refinement. Hydrogen atoms were placed in idealized positions, with C–H distances of 0.93 and 0.98 Å for aromatic and saturated carbon atoms, respectively. The isotropic thermal parameters of the hydrogen atoms were assigned the values of U_{iso} = 1.2 times the thermal parameters of the parent non-hydrogen atom.

3. Results and discussion

3.1. Synthesis and characterization

The general method for the preparation of cupric **2BB** complexes involves the reaction with the appropriate Cu^{2+} salt in equimolar amounts in refluxing methanol (Scheme 2). Isolation of microcrystalline products in the reactions with $Cu(BF_4)_2{\cdot}6H_2O$, $CuCl_2{\cdot}2H_2O$, and $Cu(OTf)_2{\cdot}6H_2O$ allowed spectroscopic characterization of the corresponding complexes. IR spectra evidence the presence of the benzimidazole groups due to the C=N stretching band around 1615 cm^{-1}, while the broad peak around 3100 cm^{-1} corresponds to the N–H stretch of the secondary amine in coordinated **2BB**. Additional characterization was carried out either by Electrospray Ionization (ESI) or Fast Atom Bombardment (FAB) mass spectrometry. For the green complex obtained from the reaction between **2BB** and $Cu(BF_4)_2{\cdot}6H_2O$, namely **[{2BBCu(μ-F)}$_2$](BF$_4$)$_2$**, ESI MS was the only technique available due to its low solubility in common organic solvents; aqueous solutions revealed the presence of a peak at *m*/*z* 396 assigned to the reduced species [**2BBCu**]$^+$, a common occurrence when benzimidazole-containing chelating ligands are employed [11]. In contrast, both products of the reactions between **2BB** and $CuCl_2{\cdot}2H_2O$ or $Cu(OTf)_2{\cdot}6H_2O$, consisting of green (**2BBCuCl$_2$**) and blue (**[2BBCu(H$_2$O)$_2$](OTf)$_2$**) microcrystals, respectively, are soluble in a variety of organic solvents. These include ethanol, methanol, and acetonitrile, thus making them amenable for FAB MS analysis: in the former case, the peak at *m*/*z* 396 consistent with the reduced species [**2BBCu**]$^+$ was also observed; in the latter case a peak at *m*/*z* 545 was detected, which was assigned to the cationic cupric complex [**2BBCu(OTf)**]$^+$.

Further characterization by X-band Electron Paramagnetic Resonance (EPR) spectroscopy was undertaken both in the solid state and in solution. The poorly soluble samples of **[{2BBCu(μ-F)}$_2$](BF$_4$)$_2$** were analyzed intially in the solid state, since

Table 1
Summary of crystallographic data.

	[{2BBCu(μ-F)}$_2$](BF$_4$)$_2$	**2BBCuCl$_2$H$_2$O**	**[2BBCu(H$_2$O)$_2$](OTf)$_2$**
Formula	$C_{40}H_{46}B_2Cu_2F_{10}N_{10}$	$C_{40}H_{46}Cl_4Cu_2N_{10}O$	$C_{22}H_{27}CuF_6N_5O_8S$
Molecular weight	1005.57	951.75	731.14
Crystal system	monoclinic	orthorhombic	monoclinic
Space group	$P2_1/n$	*Pnma*	$P2_1/n$
λ (Å)	0.71073	0.71073	0.71073
Crystal color	green	green	blue
T (K)	298(2)	298(2)	298(2)
Crystal dimensions (mm)	0.42 × 0.16 × 0.16	0.40 × 0.18 × 0.10	0.40 × 0.29 × 0.15
a (Å)	12.3882(12)	9.2032(6)	8.65590(10)
b (Å)	8.3300(8)	16.9362(12)	25.8626(3)
c (Å)	20.405(2)	14.0998(10)	13.13890(10)
α (°)	90	90	90
β (°)	102.368(2)	90	95.4710(10)
γ (°)	90	90	90
V (Å^3)	2056.8(3)	2197.7(3)	2927.93(5)
hkl ranges	$-14 \leqslant h \leqslant 14$ $-10 \leqslant k \leqslant 10$ $-24 \leqslant l \leqslant 24$	$-11 \leqslant h \leqslant 11$ $-20 \leqslant k \leqslant 20$ $-16 \leqslant l \leqslant 17$	$-10 \leqslant h \leqslant 10$ $-31 \leqslant k \leqslant 27$ $-15 \leqslant l \leqslant 15$
ρ_{calc} (g cm^{-3})	1.624	1.438	1.659
Z	2	2	4
F(000)	1028	980	1492
μ (mm^{-1})	1.125	1.255	0.981
θ range (°)	1.77–25.40	1.88–25.36	2.22–25.36
Absorption correction	empirical	empirical	empirical
T_{max}, T_{min}	0.8595, 0.6533	0.9150, 0.7625	0.9016, 0.8038
Refinement method	full-matrix least-squares on F^2	full-matrix least-squares on F^2	full-matrix least-squares on F^2
Independent reflections	3757	2080	5342
Data/restraints/parameters	3757/115/322	2080/2/143	5342/63/437
Goodness-of-fit (GOF) on F^2	1.025	1.048	1.053
R	0.0407	0.0439	0.0395
R_w	0.1089	0.1067	0.1033
Largest difference in peak, hole (e Å^{-3})	0.389, −0.239	0.791, −0.206	0.473, −0.405

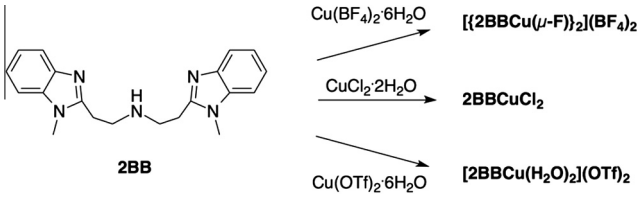

Scheme 2. Synthesis of Cu^{2+} complexes.

aqueous solutions did not provide an adequate signal. The solid samples gave rise to extremely complex signals even at 77 K, which we tentatively attribute to magnetic interactions between paramagnetic Cu^{2+} centers, consistent with a dimeric species that likely has additional magnetic coupling to the $S = ½$ ^{19}F bridging anions (see below); however poorly resolved, the axial signal observed in methanolic solution at 77 K is characteristic of isolated Cu^{2+} centers in a distorted square pyramidal environment (Fig. 1a). In contrast, the EPR spectra of either solid state or frozen acetonitrile solutions of **2BBCuCl$_2$** and **[2BBCu(H$_2$O)$_2$](OTf)$_2$** are characterized by virtually identical axial signals consistent with isolated Cu^{2+} centers in trigonal bipyramidal coordination environments ($g\perp > g_{\|}$, dz^2 ground state), based on the g values determined: $g_{\|} = 2.021$ and $g\perp = 2.157$ (Fig. 1b); the resolution of the spectra did not allow us to determine hyperfine coupling constants. The active sites of AA10 and AA11 have been described as possessing mononuclear Cu^{2+} centers in a distorted axial environment with significant $d_{x^2-y^2}$ SOMO character based on their EPR spectra [13b,c]. While the spectra of **2BBCuCl$_2$** and **[2BBCu(H$_2$O)$_2$](OTf)$_2$** differ from those determined for the metalloenzymes, the presence of the more strongly coordination fluoride in **[{2BBCu(μ-F)}$_2$](BF$_4$)$_2$** appears to favor a square pyramidal geometry in solution that more closely resembles the EPR features of AA10 and AA11.

3.2. Solid-state structures

In order to unambiguously establish the identity of all cupric complexes, their solid-state structures were determined by X-ray crystallography (Table 1). Single crystals of **[{2BBCu(μ-F)}$_2$](BF$_4$)$_2$** were obtained by slow evaporation of a concentrated aqueous solution over a period of two weeks in the monoclinic space group $P2_1/n$. The dimeric nature of **[{2BBCu(μ-F)}$_2$](BF$_4$)$_2$** was thus confirmed, accounting for its low solubility (Fig. 1). The dicopper structure is bridged by fluoride ligands, likely arising from the tetrafluoroborate counterions in the original Cu^{2+} salt. The BF_4^- anion is disordered over two positions with occupational factors of 0.58 and 0.42; the hydrogen atom of the central amine was located in the difference Fourier map, and it was refined with a restrained distance of 0.90 Å. **2BB** acts as a tridentate ligand defining a T-shape around the copper centers, similar to the N_3 donor set provided by the proteins in the active site of several PMOs. The benzimidazole N-donors are in *trans* positions relative to each other, and *cis* relative to the central amine. A first inspection of the overall coordination geometry around the Cu1 ions reveals that it is close to a square pyramid (Fig. 2). Determination of the degree of deviation from an ideal square pyramidal geometry involves the angles between *trans* ligands in the basal plane, defined as α and β, to calculate a value of $\tau = 0.08$ ($\tau = 0$ for an idealized square pyramid, $\tau = 1$ for a trigonal bipyramid) [19]. Curiously, the secondary amine N13 and F5 *trans* donors lie slightly above the basal plane (Fig. 3), whereas in most cases all basal donors are located below such plane. This results in an alternate description for the coordination geometry around the Cu^{2+} ions as capped distorted tetrahedra [20].

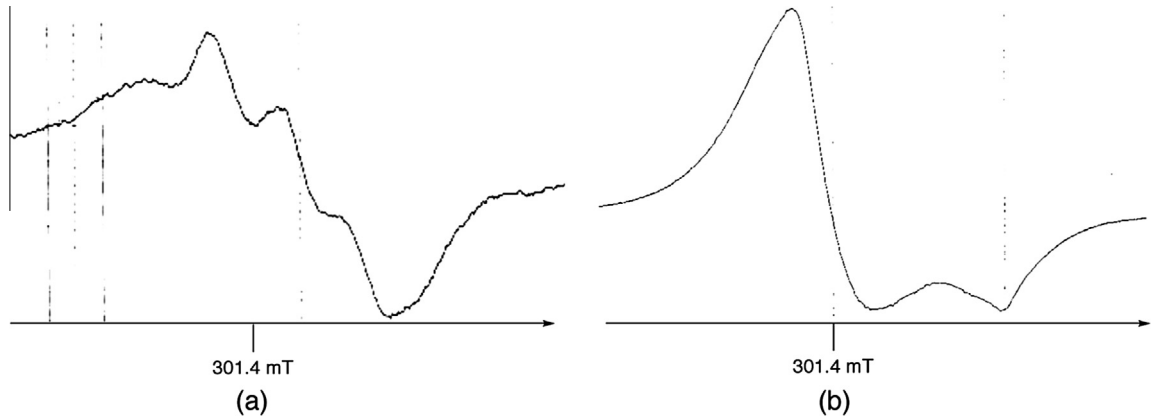

Fig. 1. EPR spectra of (a) **[{2BBCu(μ-F)}$_2$](BF$_4$)$_2$** in methanol and (b) **[2BBCu(H$_2$O)$_2$](OTf)$_2$** in acetonitrile solution.

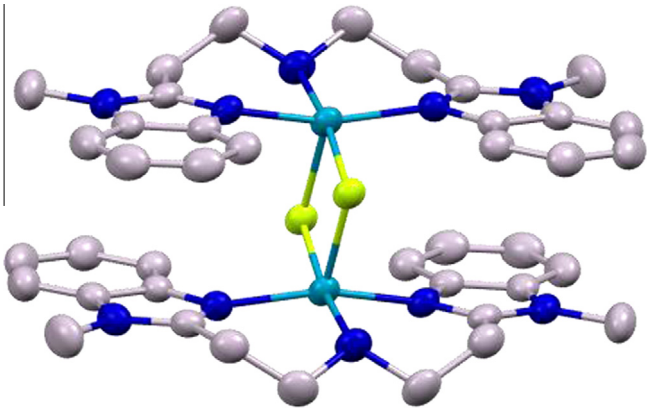

Fig. 2. Mercury diagram of **[{2BBCu(μ-F)}$_2$](BF$_4$)$_2$** at the 50% probability level; hydrogen atoms and tetrafluoroborate anions are omitted for clarity. Color code: turquoise, copper; gray, carbon; blue, nitrogen; lemon, fluorine. (For interpretation of the references to color in this figure legend, the reader is referred to the web version of this article.)

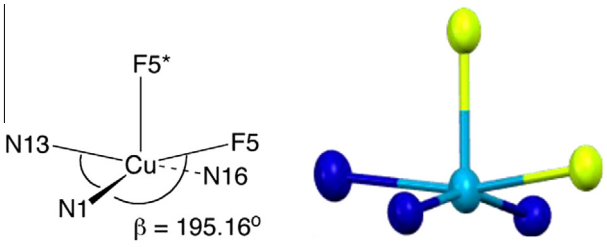

Fig. 3. Schematic representation of the coordination geometry around the Cu centers in **[{2BBCu(μ-F)}$_2$](BF$_4$)$_2$**.

X-ray quality crystals of **2BBCuCl$_2$** and **[2BBCu(H$_2$O)$_2$](OTf)$_2$** were obtained from concentrated methanolic solutions, in the former case as green prisms in the orthorhombic space group *Pnma*, and in the latter as blue crystals in the monoclinic space group $P2_1/n$. The former complex consists of a mononuclear species with a disordered molecule of H_2O in the unit cell; the latter sits at a special position, and was refined over with occupancy factors of 0.52 and 0.48 (Fig. 4). As established in frozen solution by EPR spectroscopy, the Cu^{2+} ion is in a trigonal bipyramidal coordination environment with the benzimidazole N-donors in the apical positions at a N1–Cu1–N1* angle of 175.44(16)°, and the central amine and both chlorides defining the trigonal plane, with angles ranging from 105° to 138° (Table 2). Overall, the coordination geometry

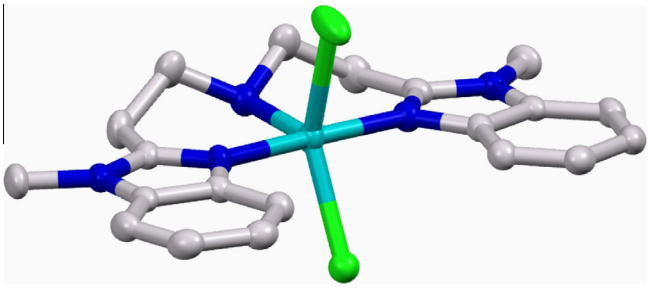

Fig. 4. Mercury diagram of **2BBCuCl$_2$** at the 50% probability level; hydrogen atoms and a molecule of H_2O are omitted for clarity. Color code: green, chlorine. (For interpretation of the references to color in this figure legend, the reader is referred to the web version of this article.)

around the cupric ion in the triflate analogue is very similar, but the chloride ligands are replaced by water molecules due to the weakly coordinating nature of the counteranions in the structure of **[2BBCu(H$_2$O)$_2$](OTf)$_2$** (Fig. 5). The CH_2NH fragment of the central amine is disordered over two positions, which were modeled with 62% and 48% occupancies. O- and N-bound hydrogen atoms were located in the Fourier map, and they were refined with restrained distances of 0.85 and 0.90 Å, respectively. The N1–Cu1–N11 angles between the apical benzimidazolic donors is 175.54(9)°, while the bond angles around the trigonal plane defined by O7, O8, and N2 vary from 117° to 123° (Table 2).

In the solid state structures determined for all cupric complexes with **2BB**, the Cu–N bond lengths to the benzimidazole donors remain relatively constant, with an average value of 1.99 Å, although the shortest in the series correspond to 1.958(2) Å in **[2BBCu(H$_2$O)$_2$](OTf)$_2$** due to electrostatic considerations; the average Cu–N distance to the central amine is 2.11 Å. Despite the fact that the coordination geometry in **2BBCuCl$_2$** and **[2BBCu(H$_2$O)$_2$](OTf)$_2$** is trigonal bipyramidal, and not tetragonal as described for the active sites of AA9–AA11 [13], the T-shape geometry imposed by the **2BB** ligand is very similar in terms of the metric parameters. The average Cu–N bond length to the histidine imidazoles is 2.0 Å, and the Cu–N bond length to the primary amine is 2.3 Å in the AA9–AA11 enzymes; the corresponding *trans* angle between the imidazole nitrogen atoms and the copper centers is close to 165°, while the angles between the cis N(imidazole)–Cu–N(amine) donors are around 97°. In the **2BB**–Cu^{2+} complexes, these angles average 170° and 92°. Moreover, the same tricoordinate mode is observed even in the reduced form of AA10 [13b], with virtually identical Cu–N distances of 2.0 and 2.3 Å for the imidazole and amine nitrogen atoms, respectively. Previous reports on the studies

Table 2
Selected bond distances (Å) and angles (°) for **[{2BBCu(μ-F)}$_2$](BF$_4$)$_2$**, **2BBCuCl$_2$**, and **[2BBCu(H$_2$O)$_2$](OTf)$_2$**.

[{2BBCu(μ-F)}$_2$](BF$_4$)$_2$			
Cu–F5	1.889(2)	F5–Cu–F5*	82.48(8)
Cu–F5*	2.225(2)	F5–Cu–N1	90.18(9)
Cu–N1	2.012(3)	F5–Cu–N13	164.85(12)
Cu–N13	2.048(3)	F5–Cu–N16	89.50(9)
Cu–N16	2.013(3)	F5*–Cu–N1	102.28(9)
		F5*–Cu–N13	82.39(11)
		F5*–Cu–N16	97.34(10)
		N1–Cu–N13	92.50(12)
		N1–Cu–N16	160.17(12)
		N13–Cu–N16	92.98(12)
		Cu–F5–Cu*	97.52(8)
2BBCuCl$_2$			
Cu1–Cl1	2.438(2)	Cl1–Cu1–Cl2	137.94(6)
Cu1–Cl2	2.369(1)	Cl1–Cu1–N1	89.03(8)
Cu1–N1	1.973(3)	Cl1–Cu1–N1*	89.03(8)
Cu1–N1*	1.973(3)	Cl1–Cu1–N2	104.70(13)
Cu1–N2	2.132(4)	Cl2–Cu1–N1	89.34(8)
		Cl2–Cu1–N1*	89.34(8)
		Cl2–Cu1–N2	117.36(12)
		N1–Cu1–N1*	175.44(16)
		N1–Cu1–N2	92.24(8)
		N1*–Cu1–N2	92.24(8)
[2BBCu(H$_2$O)$_2$](OTf)$_2$			
Cu1–O7	2.163(2)	O7–Cu1–O8	120.25(11)
Cu1–O8	2.068(2)	O7–Cu1–N1	89.27(8)
Cu1–N1	1.958(2)	O7–Cu1–N2	116.57(17)
Cu1–N2	2.152(5)	O7–Cu1–N11	88.50(8)
Cu1–N11	1.958(2)	O8–Cu1–N1	90.09(9)
		O8–Cu1–N2	123.16(18)
		O8–Cu1–N11	87.70(9)
		N1–Cu1–N2	91.74(12)
		N1–Cu1–N11	175.54(9)
		N2–Cu1–N11	92.71(12)

* Symmetry-related fluoride ligand, symmetry code: −x, −y, −z.

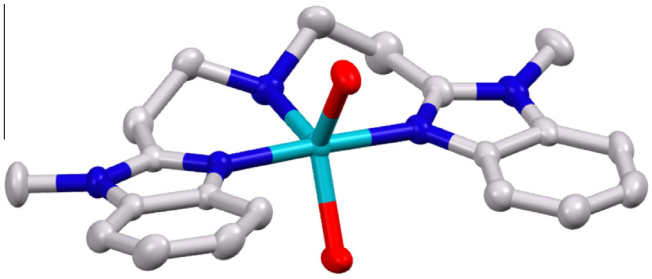

Fig. 5. Mercury diagram of **[2BBCu(H$_2$O)$_2$](OTf)$_2$** at the 50% probability level; hydrogen, minor-occupancy atoms, and triflate anions are omitted for clarity. Color code: red, oxygen. (For interpretation of the references to color in this figure legend, the reader is referred to the web version of this article.)

of related bis(benzimidazole)amine–cuprous complexes required for O_2 binding and subsequent oxygenase activity tests were hampered by the low solubility in dichloromethane of the corresponding complexes with tetrafluoroborate and hexafluorophosphate as counterions [21]. However, an initial reactivity test between **2BB** and [Cu(NCCH$_3$)$_4$]OTf in acetonitrile resulted in soluble species amenable for reactivity studies with dioxygen, which we will examine in due course.

4. Conclusions

The bis(benzimidazole)amine ligand **2BB** provides Cu^{2+} ions a coordination environment similar to that of the active sites of copper-dependent PMOs, including the N-methylated nature of the heterocyclic benzimidazole donors. The spectroscopic characterization of the cupric complexes demonstrates that the **2BB** ligand platform supports monomeric species in solution, which may be reduced with relative ease as indirectly evidenced by the detection of the [**2BBCu**]$^+$ cuprous species. In the solid state, **2BB** gives rise to either bi- or monometallic complexes, depending on the identity of the counteranions. In either case, a T-shape arrangement of the N_3 donor set is retained, structurally emulating the coordination environment in the active site of the AA9–AA11 families of PMOs provided by the histidine brace and an additional histidine imidazole. We are currently exploring the structure and reactivity of both cupric and cuprous complexes of **2BB**, and will report the results of our investigations in forthcoming work.

Acknowledgment

The authors thank Simón Hernández-Ortega for crystallographic work, Carmen Márquez and Luis Velasco for mass spectrometry measurements, María de la Paz Orta for combustion analysis, Rocío Patiño for IR determinations, Virginia Gómez-Vidales for EPR spectroscopy, CONACYT (Proyecto 151837, Beca 293842) and DGAPA-PAPIIT (IN210214) for financial support.

Appendix A. Supplementary material

CCDC 999331–999333 contain the supplementary crystallographic data for this paper. These data can be obtained free of charge from The Cambridge Crystallographic Data Centre via www.ccdc.cam.ac.uk/data_request/cif. Supplementary data associated with this article can be found, in the online version, at http://dx.doi.org/10.1016/j.ica.2014.06.027.

References

[1] (a) L.M. Mirica, X. Ottenwaelder, T.D.P. Stack, Chem. Rev. 104 (2004) 1013;
(b) E.A. Lewis, W.B. Tolman, Chem. Rev. 104 (2004) 1047;
(c) R.A. Himes, K.D. Karlin, Curr. Opin. Chem. Biol. 13 (2009) 119.
[2] (a) C. Mealli, C.S. Arcus, J.L. Wilkinson, T.J. Marks, J.A. Ibers, J. Am. Chem. Soc. 98 (1976) 711;
(b) M.R. Malachowski, H.B. Huynh, L.J. Tomlinson, R.S. Kelly, J.W. Furbee Jr., J. Chem. Soc., Dalton Trans. (1995) 31;
(c) Z. Chen, N. Karasek, D.C. Craig, S.B. Colbran, J. Chem. Soc., Dalton Trans. (2000) 3445.
[3] (a) K.D. Karlin, S. Kaderli, A.D. Zuberbühler, Acc. Chem. Res. 30 (1997) 139;
(b) S. Itoh, S. Fukuzumi, Acc. Chem. Res. 40 (2007) 592.
[4] (a) J.A. Halfern, S. Mahapatra, E.C. Wilkinson, S. Kaderli, V.G. Young Jr., L. Que Jr., A.D. Zuberbühler, W.B. Tolman, Science 271 (1996) 1397;
(b) S. Schindler, Eur. J. Inorg. Chem. (2000) 2311.
[5] D.J. Rabiger, M.M. Joullié, J. Org. Chem. 29 (1964) 476.
[6] B. Ülküseven, I. Kizilcikli, A. Tavman, B. Akkurt, Rev. Inorg. Chem. 21 (2001) 369.
[7] N.C. Li, B.E. Doody, J.M. White, J. Am. Chem. Soc. 79 (1957) 5859.
[8] (a) L.K. Thompson, B. Ramaswamy, R.D. Dawe, Can. J. Chem. 56 (1978) 1311;
(b) A.W. Addison, H.M.J. Hendriks, J. Reedijk, L.K. Thompson, Inorg. Chem. 20 (1981) 103;
(c) R. Balamurugan, M. Palaniandavar, Inorg. Chem. 40 (2001) 2246;
(d) M. Vaidyanathan, R. Balamurugan, U. Sivagnanam, M. Palaniandavar, J. Chem. Soc., Dalton Trans. (2001) 3498;
(e) R. Loganathan, S. Ramakrishnan, E. Suresh, A. Riyasdeen, M.A. Akbarsha, M. Palaniandavar, Inorg. Chem. 51 (2012) 5512.
[9] (a) L. Casella, M. Gullotti, R. Radelli, P. Di Gennaro, J. Chem. Soc., Chem. Commun. (1991) 1611;
(b) L. Casella, E. Monzani, M. Gullotti, D. Cavagnino, G. Cerina, L. Santagostini, R. Ugo, Inorg. Chem. 35 (1996) 7516;
(c) I. Garcia-Bosch, A. Company, J.R. Frisch, M. Torrent-Sucarrat, M. Cardellach, I. Gamba, M. Güell, L. Casella, L. Que Jr., X. Ribas, J.M. Luis, M. Costas, Angew. Chem. Int. Ed. 49 (2010) 2406.
[10] (a) A. Majumdar, U.-P. Apfel, Y. Jiang, P. Moënne-Loccoz, S.J. Lippard, Inorg. Chem. 53 (2014) 167;
(b) J.R. Frisch, R. McDonnell, E.V. Rybak-Akimova, L. Que Jr., Inorg. Chem. 52 (2013) 2627;
M.A.H. Moelands, S. Nijsse, E. Folkertsma, B. de Bruin, M. Lutz, A.L. Spek, R.J.M. Klein, Inorg. Chem. 52 (2013) 7394;
(d) W.-W. Yang, Y.-W. Zhong, S. Yoshikawa, J.-Y. Shao, S. Masaoka, K. Sakai, J. Yao, M. Haga, Inorg. Chem. 51 (2012) 890;
(e) M.S. Seo, N.H. Kim, K.-B. Cho, J.E. So, S.K. Park, M. Clémancey, R. Garcia-

Serres, J.-M. Latour, S. Shaik, W. Nam, Chem. Sci. 2 (2011) 1039;
(f) D. Saha, S. Das, D. Maity, S. Dutta, S. Baitalik, Inorg. Chem. 50 (2011) 46.
[11] (a) L.A. Rodríguez Solano, I. Aguiñiga, M. López-Ortíz, R. Tiburcio, A. Luviano, I. Regla, E. Santiago-Osorio, R.A. Toscano, I. Castillo, Eur. J. Inorg. Chem. (2011) 3454;
(b) I. Castillo, V.M. Ugalde-Saldívar, L.A. Rodríguez Solano, B.N. Sánchez Eguía, E. Zeglio, E. Nordlander, Dalton Trans. 41 (2012) 9394;
P.R. Martínez-Alanis, B.N. Sánchez, Chem. Eur. J. 19 (2013) 6067.
[12] (a) C.M. Phillips, W.T. Beason IV, J.H. Cate, M.A. Marletta, ACS Chem. Biol. 6 (2011) 1399;
(b) W.T. Beeson, C.M. Phillips, J.H.D. Cate, M.A. Marletta, J. Am. Chem. Soc. 134 (2012) 890.
[13] (a) R.J. Quinlan, M.D. Sweeney, L.L. Leggio, H. Otten, J.-C.N. Poulsen, K.S. Johansen, K.B.R.M. Krogh, C.I. Jorgensen, M. Tovborg, A. Anthonsen, T. Tryfona, C.P. Walter, P. Dupree, F. Xu, G.J. Davies, P.H. Walton, Proc. Natl. Acad. Sci. U.S.A. 108 (2011) 15079;
(b) G.R. Hemsworth, E.J. Taylor, R.Q. Kim, R.C. Gregory, S.J. Lewis, J.P. Turkenburg, A. Parkin, G.J. Davies, P.H. Walton, J. Am. Chem. Soc. 135 (2013) 6069;
(c) G.R. Hemsworth, B. Henrissat, G.J. Davies, P.H. Walton, Chem. Biol. 10 (2014) 122.
[14] (a) R.L. Lieberman, A.C. Rosenzweig, Nature 434 (2005) 177;
(b) R. Balasubramanian, S.M. Smith, S. Rawat, L.A. Yatsunyk, T.L. Stemmler, Nature 465 (2010) 115.
[15] L. Casella, E. Monzani, M. Gullotti, F. Gliubich, L. De Gioia, J. Chem. Soc., Dalton Trans. (1994) 3203.
[16] Bruker AXS, SAINT Software Reference Manual v. 6.23C, Madison, 2002.
[17] G.M. Sheldrick, SHELXS-97, Crystal Structure Solution, University of Göttingen, Germany, 1990.
[18] G.M. Sheldrick, SHELXL-97, Crystal Structure Refinement, University of Göttingen, Germany, 1997.
[19] A.W. Addison, T.N. Rao, J. Reedijk, J. van Rijn, G.C. Verschoor, J. Chem. Soc., Dalton Trans. (1984) 1349.
[20] C. Lee, C. Mellot-Draznieks, B. Slater, G. Wu, W.T.A. Harrison, C.N.R. Rao, A.K. Cheetham, Chem. Commun. (2006) 2687.
[21] T.N. Sorrell, M.L. Garrity, Inorg. Chem. 30 (1991) 210.